small
NANO MICRO

How Do the Electrical Properties of Graphene Change with its Functionalization?

*T. S. Sreeprasad and Vikas Berry**

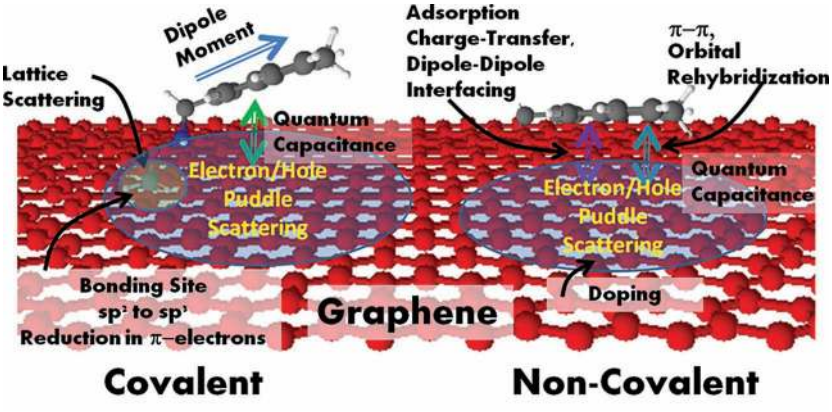

From the Contents

Functionalization of graphene is essential to interface it with other moieties to expand the scope of its electrical/electronic applications. However, chemical functionalization and/or molecular interactions on graphene sensitively modulate its electrical properties. To evaluate and take advantage of the properties of functionalized graphene, it is important to understand how its electrical attributes (such as carrier scattering, carrier concentration, charge polarity, quantum-capacitance enhanced doping, energy levels, transport mechanisms, and orbital hybridization of energy-bands) are influenced by a change in carbon's structural conformation, hybridization state, chemical potential, local energy levels, and dopant/interface coupling induced via functionalization or molecular interactions. Here, a detailed and integrated model describes factors influencing these electrical characteristics of functionalized graphene (covalent bonds, adsorption, π–π bonds, and lattice incorporation). The electrical properties are governed via three mechanisms: (a) conversion of carbon's hybridized state, (b) dipole interactions enhanced via quantum capacitance, and (c) orbital hybridization with an interfacing molecule. A few graphenic materials are also identified where further studies are essential to understand the effect of their functionalization.

1. Introduction

Isolated from graphite for the first time in 2004,[1] graphene is a single atom thick 2D sheet of sp^2-hybridized (double-bonded) carbon atoms arranged in a honeycomb lattice. Electronically, graphene is a semimetal with zero bandgap owing to the conduction band touching the valence band at two points (K and K') in the Brillouin zone.[1–4] Graphene exhibits the highest room-temperature carrier mobility[5–8] measured for any material, a high optical absorptivity (2.3%),[9] high thermal conductivity (25 times that of silicon),[10] and high mechanical strength (it is the strongest nanomaterial).[11] For several applications it is important that graphene be functionalized.[12,13] These include high-specificity sensors, transistors fabricated with atomic layer deposition (ALD) for top-gating, and optoelectronic devices created by interfacing graphene with dye molecules or quantum dots. Therefore, it is important to understand the change in graphene's electrical properties, which are influenced by its functionalization and molecular interactions. The current reviews on the electrical properties of functionalized graphene have not produced a unified model for the functionalization/electrical attributes of graphene.[14–23] This review outlines an integrated model describing the mechanisms linking several functionalization events to the electrical properties of functionalized graphene (**Figure 1**).

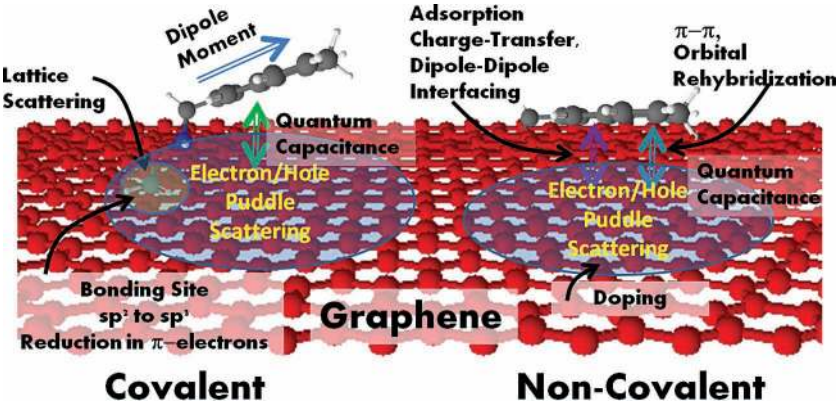

Figure 1. A schematic of the effect of functionalization (covalent and non-covalent) on the electrical attributes (charge density, scattering, electron–hole puddle size/density, doping) due to a change in carbon's hybridization state, graphene's quantum capacitance, lattice distortion, charge transfer, dipole–dipole interfacing, and orbital hydridization.

2. Interplay Between Functionalization and Electrical Properties

Functionalization and/or molecular interfacing of graphene sensitively modulates its electrical properties.[24] In order to explain the correlation between functionalization and electrical properties, we list the functionalization-related phenomena, which directly influence graphene's electrical attributes: (a) conversion of the hybridization state of carbon atoms,[25] (b) creation of a barrier at the functionalization site and within the electron-potential continuum,[24] (c) distortion of its 2D planar lattice,[25] (d) molecular-dipole-induced doping,[26] (e) amplified change in the density-of-states due to graphene's high quantum capacitance[26,27] ($C_Q = 4e\pi^{1/2}/h\vartheta_F(n_l)^{1/2}$ - see Section 4),[12] (f) hybridization of the molecular orbitals with graphene,[28] (g) lattice incorporation and/or defects on graphene,[29] (h) introduction of new energy levels,[30] and (i) introduction of strong edge states and quantum confinement via structural constraints (nanoribbons, quantum dots, nanomesh).[31] In addition, the electrical properties change as a result of the Schottky barrier produced via transfer of charges from the electrode to graphene and vice versa due to different work functions. These modifications in the chemical, electronic, and structural construct of graphene (Figure 1) can be caused by molecular functionalization/interaction at graphene sites occurring via (1) covalent bonding, (2) π–π interfacing, (3) physisorption, or (4) lattice substitution. Direct covalent functionalization of an sp^2-hybridized carbon in graphene converts it into a tetrahedral sp^3-hybridized carbon, which causes a loss of the free, sp^2-associated π electron constituting the π-cloud on graphene. On the other hand, atomic substitution of carbon with another element (such as N or B) retains the sp^2 character; however, it disrupts the π–cloud continuum due to the addition or removal of an electronic state through the (more electropositive or electronegative) substituting element. It is important to note that non-covalent functionalization of graphene via physisorption or π–π interfacing does not distort the sp^2 network; however, it changes the doping density, increases the density of electron–hole puddles, and creates scattering sites. Also, the widely employed solution-gating of graphene exploits the short distance of electric-double-layer potential to effectively dope graphene. This review discusses the mechanisms of changes in electrical properties caused by different functionalization schemes, followed by a combined model for these functionalization routes. We do not discuss the change in electrical properties due to vacancy defects or in graphene quantum structures.[31]

3. Covalently Functionalized Graphene

3.1. Electrical Properties of Covalently Functionalized Graphene

Covalent functionalization is the most studied form of graphene functionalization, and probably causes the most significant changes to graphene's electrical properties. Graphene

Dr. T. S. Sreeprasad, Prof. V. Berry
Department of Chemical Engineering
Kansas State University
Manhattan, Kansas 66506, USA
Website: http://www.che.ksu.edu/~vberry/index.html
E-mail: vberry@ksu.edu

DOI: 10.1002/smll.201202196

NANO MICRO small

oxide (GO) and reduced graphene oxide (RGO) are the most commonly studied graphenic structures. Reducing GO produces RGO; however, RGO invariably consists of unreduced, covalently bonded oxy groups.[32] Covalent functionalization of a carbon atom on graphene converts the planar sp^2 lattice-point into a tetrahedral sp^3 lattice-point (**Figure 2**), which breaks the potential continuum via creation of a quantum well, leading to the introduction of a scattering site in graphene. Further, the removal of the π electron from the carbon atom reduces the carrier density and can introduce a bandgap (via removal of electronic states) and/or a transport barrier. The functionalizing molecule can also introduce energy levels (edge states and functionalization states) in the band structure of covalently functionalized graphene (CFG) to make it an n-type or p-type semiconductor. Therefore, a combination of the carrier deficiency at the sp^3 site, the associated disruption of the electron-potential continuum, and the distorted planar lattice causes a drastic reduction in graphene's carrier mobility and a change in charge polarity/density. For example, in comparison to graphene (room temperature mobility = 10 000–50 000 $cm^2/V/s$ and intrinsic mobility limit 200 000 $cm^2/V/s$), RGO, with few residual oxy groups, exhibits a drastically reduced carrier mobility (0.05–200 $cm^2/V/s$), p-type behavior, and a finite effective bandgap[33–35] of 0.2 to 2 eV.[36,37] It is important to note that a more accurate depiction of a functionalization-induced band structure change can be predicted by density functional theory and Green's function simulations, which are not discussed in this review.

Charge transport depends on whether the functionalization of graphene (a) forms domains or (b) is dispersed. Several studies have shown evidence of the coexistence of two domains containing sp^2 (graphenic region with a low bandgap) and sp^3 (functionalized region with high bandgap) regions in some FGs, for example GO.[30] Here, there is a separation between the sp^2 graphenic region (which exhibits high-conductivity (Klein tunneling)[38]) and the sp^3 region (which exhibits insulating or semi-conducting properties).[25]

T. S. Sreeprasad is a postdoctoral fellow at the Kansas State University. He earned his PhD from the Indian Institute of Technology, Madras, in 2011 and MS from the School of Chemical Sciences, MG University. His areas of interest include nanosystems and 2D materials.

Vikas Berry is the William H. Honstead professor of chemical engineering and associate professor at Kansas State University. He received his PhD from Virginia Tech in 2006, MS from KU in 2002, and BS from IIT-Delhi in 1999. Amongst his honors is the NSF-CAREER award. His current areas of research interest include graphene science and technology, bio-nanotechnology, and molecular electronics.

Since the sizes of these domains have a wide distribution, the carrier transport from one sp^2 region to another of different sizes, shapes, and varying transport barriers occurs via variable-range hopping (**Figure 3**). This charge transport is given by: $I = I_0\ exp(-(T_0/T)^{1/3})$, where the exponent 1/3 represents transport in 2D. Further, the smaller sp^2 region shows quantum confinement-induced semiconducting behavior. On the other hand, the dispersed functionalization leads to a reduction in the mean free path and Fermi velocity, and an increase in elastic and inelastic scattering.[39] Also, while graphene sheets contain electron–hole puddles due to inherent structural imperfections,[40] these electron–hole puddles are sensitively influenced by functionalization[41] and act as scattering centers during transport. Interestingly, the electron–hole puddles in turn influence the functionalization of graphene.

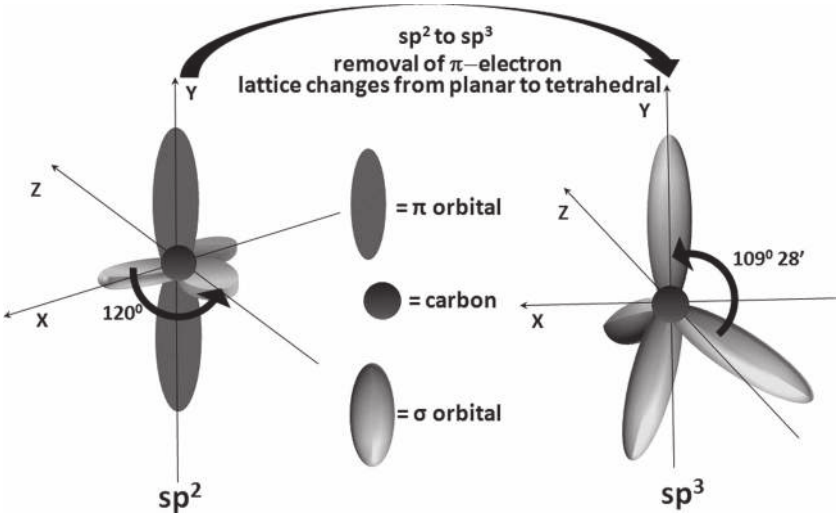

Figure 2. (A) Schematic representation of the effect of change in hybridization of carbon. Conversion of sp^2 to sp^3 leads to removal of the π electron and conversion of the planar lattice to tetrahedral.

3.2. Covalent Functionalization of Graphene

Being highly inert and thermally stable, graphene requires high-energy processes to rehybridize its π-conjugated carbon network. The most commonly used strategy to functionalize graphene is oxidation of graphite and its exfoliation in acid[42] to produce graphene oxide (GO), with oxygenated organic functionalities such as

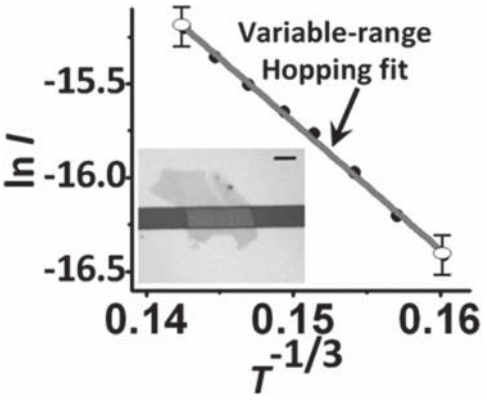

Figure 3. Plot showing the variable-range hopping exhibited by an RGO sample from our lab. The optical image of the device used for the measurment is also given.

carboxyl, epoxy, hydroxyl, carbonyl, phenol, lactone, and quinine.[43] This results in the formation of a large density of sp^3-hybridized carbons in the graphene network,[44] which disrupts the delocalized π cloud, converting graphene into an insulator.

The oxidation of graphite was first conducted by B. C. Bordie in 1859[45] and later by Hummer, where graphite was oxidized using potassium permanganate and sulfuric acid, which is currently the most commonly used process.[42] Here, Mn_2O_7 is responsible for the oxidation of aliphatic double bonds in aromatic rings.[46] In acidic conditions (i.e., in the presence of H_2SO_4), MnO_4^- reacts with a transient species MnO_3^+ to produce Mn_2O_7 via the following reactions:

$$3H_2SO_4 + KMnO_4 \rightarrow 3HSO_4^- + K^+ + H_3O^+ + MnO_3^+$$

$$MnO_3^+ + MnO_4^- \rightarrow Mn_2O_7$$

In these reactions, MnO_4^- can react with unsaturated double bonds and cleave them to produce aldehydes or ketone structures or to oxidize the double bond to produce diols. The aldehydes can be further oxidized to carboxylic acid groups. Dehydration of diols can result in the formation of epoxides. Hence, a large variety of functionalities such as carboxyl, carboxylic acid, hydroxyl, and ether are formed on the graphene surface. These oxy groups can be further functionalized with other molecular species via condensation, electrophilic/nucleophilc substitution, and addition reactions, as depicted in **Figure 4** and **Table 1**. These reactions are discussed in the next section.

Table 1. Different strategies for covalent functionalization of graphene categorized based on the mechanism.

Mechanism of functionalization	Functionalizing molecules
Condensation reaction	Octadecyl amine,[49] amine-functionalized poly(ethylene glycol),[50] triphenylamine-based polyazomethine,[51] amine-functionalized porphyrin,[52] amino acids and protein (adenine, cystine, nicotamide, ovalbumin) and propyl amine,[53] concanavalin A,[54,55] isocyanates,[56] diisocyanates,[57] oligoester using toluene-2,4-diisocynate,[58] β-cyclodextrin,[59] poly(vinyl alcohol),[60] and alkylchlorosilanes in the presence of butylamine and toluene.[61]
Nucleophilic substitution reaction	Dodecyl amine,[62] 4,4′-diaminodiphenyl ether,[63] poly(oxyalkylene) amines,[64] allylamine (solvothermal reaction),[65] 4-aminobenzenesulfonic acid,[63] poly-L-lysine,[66] polyethylene,[67] dopamine,[68] polyglycerol,[69] poly(norepinephrine),[70] 6-amino-4-hydroxy-2-naphthalenesulfonic acid,[71] 3-aminopropyltriethoxysilane,[72] amine-terminated ionic liquids,[73] and epoxidized methyl oleate.[74]
Electrophilic substitution reaction	Diazonium salts of para-nitro aniline,[75] 4-bromoaniline,[76] sulfanilic acid,[77] and aryl diazonium salt (on surfactant-wrapped graphene),[48,78] polystyrene,[79]
Addition reaction (including cycloaddition)	*N*-methyl-2-pyrrolidone.[80] Several Diels-Alder type reactions,[81] azomethine ylide,[82,83] azidotrimethylsilane,[84] polyacetylene,[85] aryne,[86] cyclopropanated malonate,[87] alkylazides.[88]

3.3. GO Functionalization

Functionalization or chemical modification of the oxy groups on GO can lead to molecular (dipole–dipole) interactions with graphene to further change its electrical properties.

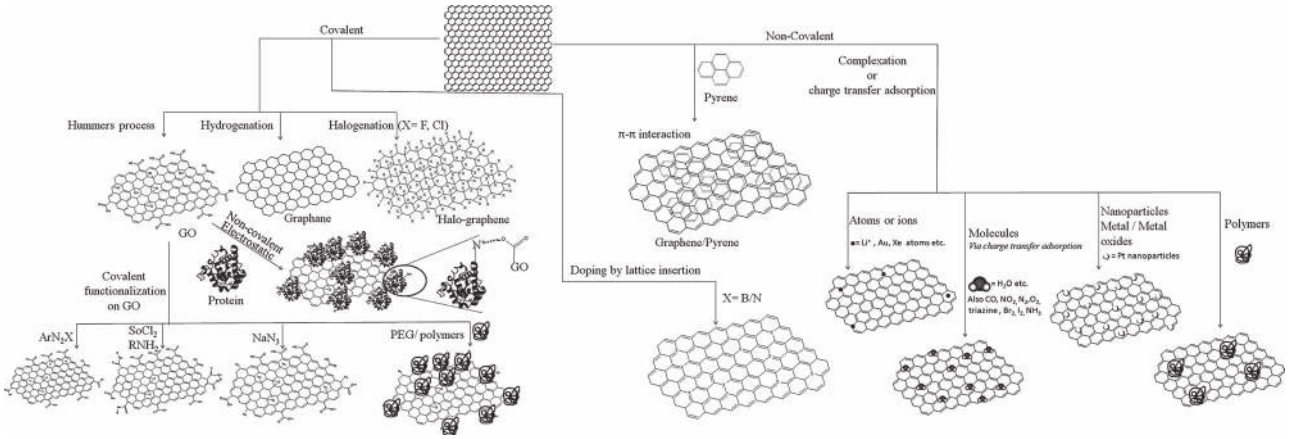

Figure 4. Schematic showing various functionalization routes of graphene.

NANO MICRO small

For example, the amine compounds isocyanate and diisocyanate react with GO by forming amides and carbamate ester linkages (condensation reactions, Table 1), which changes GO's carrier density and polarity. Similarly, in nucleophilic substitution reactions, molecules with electron lone pairs (e.g., amines) attack epoxides (nucleophilic centers) on GO.[47] Here, a wide variety of moieties with different dipole moments and electronegativities can be grafted onto graphene (Table 1). Electrophilic substitution reactions require displacement of a hydrogen atom from GO by an electrophile. Here, functionalization with aryl diazonium salts is the most feasible reaction,[48] which follows a free-radical mechanism via an electrochemical reduction process known as the Saevant method (Table 1). In cycloaddition reactions (Diels-Alder reactions, [2 + 1] cycloaddition, and nitrene mediated reactions), unsaturated molecules combine to form a cyclic moiety with graphene (Table 1).

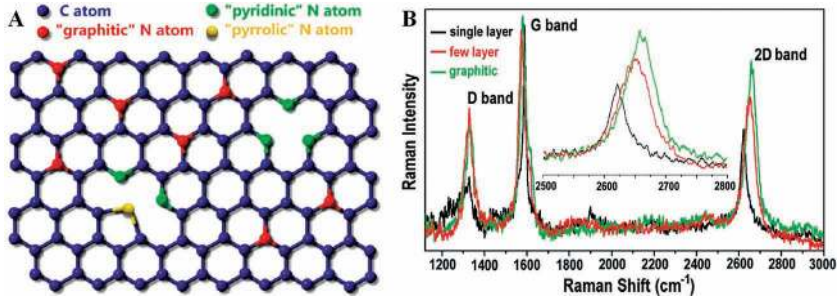

Figure 5. A) Schematic representation of the N-doped graphene where the blue, red, green, and yellow spheres represent the C, "graphitic" N, "pyridinic" N, and "pyrrolic" N respectively. B) Raman spectra of the N-doped graphene. The green, red, and black lines correspond to the graphite-like, few-layer, and single-layer graphene, respectively. Enlarged spectra of the 2D band (inset). Adapted with permission.[29] Copyright 2009, American Chemical Society.

3.4. Plasma-Induced Functionalization

Functionalization of graphene with species generated via plasmas is gaining significant attention due to the ease and versatility of the process. For example, the electrical properties of graphene can be changed significantly by hydrogenating (reducing) sp^2 graphene into sp^3 graphane containing saturated bonds via plasma-generated atomic hydrogen.[25] Here, graphane (on silica) exhibits a p-type behavior and 5.4 eV bandgap;[89] however, hydrogen adsorbed over graphene on an Ir(111) substrate results in the opening of a bandgap (450 meV) near the Fermi level.[90] Fluorine and chlorine are other highly reactive species which can functionalize graphene via a similar mechanism to make it strongly insulating (graphene–fluoride resistance > 10 ΓΩ at room temperature). Graphene can be fluorinated via XeF_2[91,92] or fluorine gas at 600 °C,[93] and chlorinated via photochemical chlorination[94] or chlorine plasma.[95] Unlike hydrogen and fluorine plasmas, slower reaction kinetics between the chlorine plasma and graphene allow a controlled and non-destructive chlorination.

3.5. Atomic Incorporation into the Graphene Lattice and Consequent Electrical Properties

Graphene can be n- or p-doped via direct atomic incorporation of electropositive or electronegative elements on its lattice (a) during its growth via chemical vapor deposition (CVD) or (b) by ion-radiation-induced vacancy creation and doping. CVD has been employed extensively to produce monolayer graphene on metal foils from fluidic or solid carbon sources such as methane (CH_4) or poly(methyl methacrylate) (PMMA) in the presence of hydrogen, which catalytically[96] strips hydrogen atoms from the carbon source, producing reactive carbon which binds to produce graphene (on a surface or during precipitation). The dopant can be introduced during CVD growth. For example, Wei et al.[29] used ammonia (NH_3) as a nitrogen source along with CH_4 (1:1 ratio) in CVD to produce N-doped graphene with ~8.9% nitrogen incorporated via lattice substitution. A smaller fraction was incorporated as pyridinic or pyrrolic nitrogen, as shown in **Figure 5**A. In these forms, the nitrogen is present in the π-conjugated system or contributes electrons to the π system, respectively. As shown in the Raman spectra in Figure 5B, the doping leads to a shift in the 2D peak. All samples after N-doping show prominent D peaks, indicating the large number of topological defects created. The gating measurements on the N-doped graphene exhibit n-type conductivity with a high ON-OFF ratio, up to 3 orders of magnitude. However, the doping leads to reduction of the carrier mobility of graphene by ~30%, probably due to the breakage of the potential continuum at the lattice-incorporation sites. In the case of ion irradiation, Guo et al.[97] showed that reversible vacancy defects can be produced on pristine graphene via irradiation with different dosages of N^+ ions. These defects produced highly reactive carbon sites, which could be annealed back to a graphene lattice. However, exposure of the defected graphene to ammonia (NH_3) at high temperature incorporated nitrogen into the graphene's defect sites, producing n-type N-doped graphene, as confirmed by a negative Dirac voltage (V_{Dirac}). The carrier mobility of the N-doped graphene was measured to be ~6000 $cm^2/V/s$. Similarly, boron can be doped into the graphene lattice via CVD to produce a p-type graphenic sheet.[98]

4. Electrical Properties of Non-Covalently Functionalized Graphene

Molecules interfacing (π–π or adsorbed) on graphene do not distort its lattice; however, quantum coupling of the interfaced molecules enhances the effective electric field on graphene due to the dipole moment of the molecule (**Figure 6**). This in turn introduces scattering sites by changing the local potential at the attachment site, or by creation of high-density electron–hole puddles). Here, the density of states in graphene

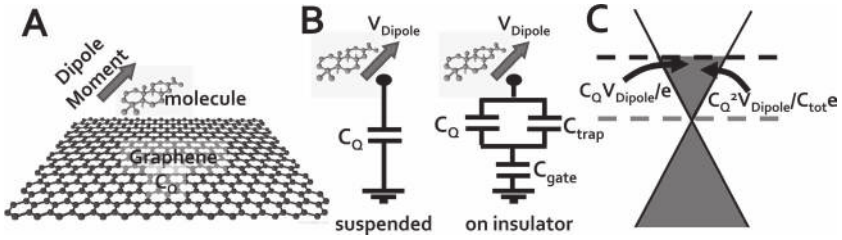

Figure 6. A) Schematic of a molecule interfacing with graphene, where the molecular dipole moment applies a voltage V_{Dipole} to graphene. Here, graphene could be suspended and have a total capacitance of C_Q, its quantum capacitance, or it could be on an insulator and have a gate capacitance of C_G and trap capacitance of C_{Trap}. B) The capacitance circuit for suspended or surface-immobilized graphene with voltage = V_{Dipole}. C) The charge density induced in graphene due to molecular interfacing will be $n = C_QV_{Dipole}/e$ (suspended) and $C_Q^2V_{Dipole}/C_{tot}e$ (on insulator). Electron doping is illustrated here.

is significantly changed due to its high quantum capacitance (given by $C_Q = 4e\pi^{1/2}/h\vartheta_F(n_l)^{1/2}$, where e is the electronic charge, h is Planck's constant, ϑ_F is the Fermi velocity of the Dirac electron, and n_l is the intrinsic carrier concentration of graphene. **Figure 7**A shows simulated results of the increase in C_Q with an increase in intrinsic carrier densities (n_l) and doping levels (n∗). The simulated result indicates that, as n∗ increases, the minimum capacitance value decreases. These trends were confirmed by measuring the total capacitance and the quantum capacitance of graphene in an ionic liquid (BMIM-PF_6), as shown in Figure 7B.

The quantum capacitance leads to enhanced effective gating (ΔV_G) from the interfaced molecules. ΔV_G due to the dipole voltage (V_{Dipole}) of the molecule is given by $\Delta C_G = (C_Q/C_{tot})V_{Dipole}$. Here, $C_{tot} = (C^{-1}_Q + C^{-1}_g)^{-1}$ and C_g is the gate capacitance. Therefore, due to the quantum capacitance in graphene, the density of states is directly amplified by the interfaced molecule's dipole moment and is given by $(C_Q/e)V_{Dipole}$ for suspended graphene and $(C^2_Q/eC_{tot})V_{Dipole}$ for substrate-immobilized graphene.

Further, doping graphene with electron-withdrawing groups creates a hole-rich graphene, while electron-donating functionalities create electron-rich graphene. Similarly, adsorbing metal atoms with high electron affinity (e.g., gold atom adsorption[99]) on graphene produces p-type graphene, while alkali metal adsorption (with electron-donating capabilities, e.g., Li, Na) produces n-type graphene by forming ionic bonds between graphene and these metals.[100,101] Doping can also alter the electronic structure of graphene through a charge transfer from/to the electron-donor and/or electron-acceptor molecules. Some examples where changes in the electrical properties of graphene has been observed include: (a) pyrene molecules attached on both sides opening up a bandgap,[102] (b) controlled adsorption of water molecules inducing a bandgap of ~0.206 eV,[103] and (c) adsorption of (2,2,6,6-tetramethylpiperidin-1-yl)oxidanyl (TEMPO) through NO radicals making graphene an n-type semiconductor.[104] For π–π functionalization with aromatic molecules, hybridization of the molecular orbital/s with graphene's valence band occurs, where the net effect is the conversion of the semi-metallic graphene to a metallic graphene. In all systems, the change in carrier density (Δq) due to functionalization can be calculated by measuring the change in the mobility and density. For back-gating studies: $\mu_{carrier} = (\Delta I_{DS}/\Delta V_G)/(C_G(l/w)V_{DS})$, where $\mu_{carrier}$ is mobility of carriers. The carrier density can be measured via silicon back-gating studies or Hall measurements. Graphene's bandgap can be measured electrically by variable temperature measurements[6] from 4 to 300 K for sheets or conductivity/gating analysis[37] for sheets, or by On/Off rectification ratio[105] and gating studies.[37]

4.1. Non-Covalent Functionalization of Graphene

Non-covalent functionalization routes for graphene include van der Waals interactions and π–π stacking of aromatic molecules on graphene. These forms of functionalization do not disrupt the extended π conjugation on graphene and do not create sp^3-hybridized carbons or defects. Polycyclic aromatic compounds like pyrene, perylene, anthracene, triphenylene, and coronene (and graphene) can bond with one another via π–orbital overlapping to form a π–π interface, which is stronger than hydrogen bonding, van der Waals, or dipole–dipole interactions (though not as strong as covalent bonds). Therefore, most aromatic molecules exhibit π–π interactions with graphene and can tune the electron density of the hybrid system via orbital hybridization. These are the interactions responsible for keeping graphene layers together in graphite. The higher the number of rings involved, the stronger the π–π interaction. As an example, using pyrene-1-sulfonic acid sodium salt (PyS)[106] as the electron donor and the disodium salt of 3,4,9,10-perylenetetracarboxylic diimide bisbenzenesulfonic acid (PDI) as the electron acceptor, a donor–acceptor complex can be fabricated on graphene, since PyS and PDI have large planar aromatic structures.[107] Other examples of π–π interactions include functionalization of

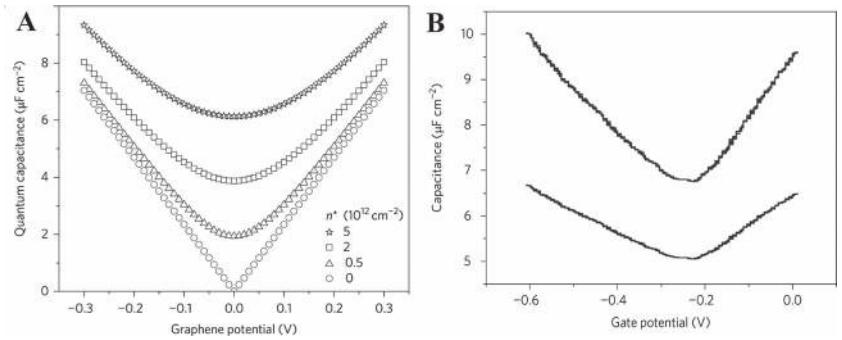

Figure 7. A) Simulated quantum capacitance of graphene at different effective charged impurities n∗. B) Total capacitance (bottom trace) and quantum-capacitance (top trace) of graphene measured in ionic liquid BMIM-PF_6 as a function of gate potential. Adapted with permission.[27] Copyright 2009, Nature Publishing Group.

NANO MICRO small

picket-fence porphyrin (FeTMAPP),[108] pyrenebutyrate,[109] porphyrin (5,10,15,20-tetrakis(1-methyl-4-pyridinio)porphyrin (TMPyP)),[110] coronene carboxylate,[111] and polyoxyethylene sorbitan laurate.[112] Further adsorption-based anchoring of polymers on graphene has been achieved with ethyl cellulose,[113] 1,2-distearoyl-sn-glycero- 3-phosphoethanolamine-*N*-[methoxy(polyethyleneglycol)-5000] (DSPE-mPEG)[114] and poly(m-phenylenevinyleneco-2,5-dioctoxy-p-phenylenevinylene) (PmPV),[115] PMMA,[116] poly(3-hexylthiophene-2,5-diyl) (P3HT) and poly[2-methoxy-5-(2-ethylhexyloxy)-1,4-phenylenevinylene] (MEH-PPV).[117] Here, the interfacing molecule's dipole moment and the enhanced doping due to the high quantum capacitance of graphene sensitively changes graphene's electrical properties.[118] Another example of non-covalent binding is that between oxygen functionalities (named 'oxygen debris') and the sp^2 lattice region of GO. Here, the oxygen can be detached under basic conditions.[119]

4.2. Gas Adsorption

Gas molecules adsorbed on graphene induce a significant change in its electrical behavior. Adsorption of NO, NO_2, NH_3, H_2O, H_2, and CO[120–125] molecules can act as donors or acceptors, resulting in sensitive doping and changes to graphene's electrical conductivity. Graphene—being a perfect 2D crystalline material which can be considered as having only a surface and no volume, with exceptional conductivity even in the limit of zero carrier density—will have significant fluctuations in relative carrier concentration by the addition of a few extra electrons.[120,121,125–129] This molecular doping can follow two charge-transfer mechanisms: (a) charge transfer can happen depending upon the relative positions of the highest occupied molecular orbital (HOMO) and lowest unoccupied molecular orbital (LUMO) of the adsorbate with respect to the Fermi level of graphene in the density of states. If the Fermi level of pristine graphene is below the HOMO of the adsorbate in density of states, there is a charge transfer towards graphene. However, if the Fermi level of graphene is close to the LUMO of the adsorbate which is situated below the Fermi level, the charge transfer will be towards the adsorbate molecule; (b) the orbital hybridization of the HOMO and LUMO with graphene can also influence the charge-transfer process. There is an inverse relationship between energy difference between the interacting orbital and the extent of hybridization.

5. Integrated Model for Mechanism

Based on the review above, we propose three fundamental mechanisms (or effects) of functionalization, which affect the electrical properties of graphene post functionalization. These are (a) conversion of the basal carbon's hybridization state (sp^2 to sp^3), which distorts the lattice, disrupts the potential continuum, enhances electron–hole puddles, and changes the density of electronic states; (b) interaction of the dipole moment of the functionalizing/interfacing molecules with graphene, which leads to enhanced doping due to quantum capacitance, increase in electron–hole puddles, and disruption of the potential continuum, and; (c) molecular orbital hybridization with graphene's electronic bands. For covalent functionalization, the electrical properties are influenced by all of the above three mechanisms. For molecular adsorption and aromatic π–π interactions, a combination of mechanisms (b) and (c) occurs. Two other functionalization schemes which affect electrical properties are (1) introduction of defects, and (2) lattice incorporation. The defect acts as a carrier-deficient center and lattice-distortion site, which causes scattering (similar to the mechanism (a) mentioned above). The lattice incorporation of a dopant might not create a lattice distortion; however, it will lead to breakage of the potential continuum and enhanced electron–hole puddles, which will lead to enhanced scattering. The dopant polarity is governed by the bonding mechanism, molecular dipole moment, and its electronegativity; the mobility is governed by functionalization density, electronegativity (creation of an electron–hole puddle), the bonding/interfacing mechanism (lattice distortion and potential continuum), and sp^2/sp^3 domain sizes; and the transport mechanism is governed by sp^2/sp^3 domain-size distribution, and the bonding/interfacing mechanism (potential barrier for transport and electron–hole puddle distribution). The same mechanism can describe the electrical properties of graphene/nanoparticle hybrids as well.[130–132]

6. Future Scope for Research

While graphene functionalization has gained significant attention, relatively limited knowledge is available on the effect of functionalization on sandwiched graphene sheets, such as graphene bilayers with only one layer functionalized or graphene trilayers with both outer layers functionalized. Here, it is expected that the electrical properties will be influenced by π–π bonding, orbital hybridization, and quantum-capacitance-induced doping (via dipole moments from the functionalized layer), however, experimental evidence is required. Importantly, the electron–hole puddle-induced scattering will have to be studied. It is important to note that such structures are challenging to fabricate and control. Another category of graphenic materials gaining attention is graphene nanostructures, such as graphene quantum dots (GQDs) and graphene nanoribbons (GNRs) which, due to quantum confinement (<100 nm for GQDs and <50 nm for GNRs) and edge states, open a bandgap. For these nanostructures, it is important to study the combined effects of quantum confinement and functionalization on their band structure. Further, the dimensions of the electron or hole puddles (usually several micrometers in graphene), if any, in these nanostructures will have to be evaluated, especially for GNRs, which are considered to be the ideal graphene-based material for transistors.

A recent study showed that functionalization on graphene depends on the electron–hole puddles, which can significantly alter both the Fermi level and the scattering-center density to produce multifunctional graphene sheets.[133] Such multifunctional sheets with organized functionalized and

non-functionalized domains need to be studied for their electronic transport properties. Similarly, graphene/boron-nitride hetrostructures also need to be studied for their electrical transport properties. Further, there is scope to conduct detailed studies on the creation of electron–hole puddles on graphene as a consequence of molecular interfacing and functionalization. These could be scanning tunneling microscopy (STM) experiments, which can locate the molecular attachment site and map the electron–hole puddles around the site.

7. Summary

This review outlines a detailed and integrated model to explain the factors influencing the electrical properties of functionalized graphene (covalent bonding, adsorption, π–π interactions, and lattice incorporation). The model explains that the electrical properties are governed via three mechanisms: (a) conversion of the sp^2-hybridized state to sp^3, (b) molecular dipole interactions and the associated quantum-capacitance-enhanced doping, and (c) hybridization of molecular orbitals with graphene's electronic bands. Also, graphene trilayers with outer layers functionalized, graphene quantum structures, and multi-functionalized graphene are identified as upcoming graphenic materials where further functionalization/electrical studies are required.

Acknowledgements

VB thanks the financial support from NSF (CMMI-1054877, CMMI-0939523 and CMMI-1030963), Office of Naval Research (grant-N000141110767), Terry C. Johnson Center for Basic Cancer Research, and KSU start-up.

[1] K. S. Novoselov, A. K. Geim, S. V. Morozov, D. Jiang, Y. Zhang, S. V. Dubonos, I. V. Grigorieva, A. A. Firsov, *Science* **2004**, *306*, 666.
[2] K. S. Novoselov, E. McCann, S. V. Morozov, V. I. Fal'ko, M. I. Katsnelson, U. Zeitler, D. Jiang, F. Schedin, A. K. Geim, *Nat. Phys.* **2006**, *2*, 177.
[3] K. S. Novoselov, A. K. Geim, S. V. Morozov, D. Jiang, M. I. Katsnelson, I. V. Grigorieva, S. V. Dubonos, A. A. Firsov, *Nature* **2005**, *438*, 197.
[4] K. S. Novoselov, D. Jiang, F. Schedin, T. J. Booth, V. V. Khotkevich, S. V. Morozov, A. K. Geim, *Proc. Natl. Acad. Sci. USA* **2005**, *102*, 10451.
[5] M. H. Gass, U. Bangert, A. L. Bleloch, P. Wang, R. R. Nair, A. K. Geim, *Nat. Nanotechnol.* **2008**, *3*, 676.
[6] X. Du, I. Skachko, A. Barker, E. Y. Andrei, *Nat. Nanotechnol.* **2008**, *3*, 491.
[7] J. H. Chen, C. Jang, S. D. Xiao, M. Ishigami, M. S. Fuhrer, *Nat. Nanotechnol.* **2008**, *3*, 206.
[8] A. Akturk, N. Goldsman, *J. Appl. Phys.* **2008**, *103*, 053702.
[9] R. R. Nair, P. Blake, A. N. Grigorenko, K. S. Novoselov, T. J. Booth, T. Stauber, N. M. R. Peres, A. K. Geim, *Science* **2008**, *320*, 1308.
[10] A. A. Balandin, S. Ghosh, W. Bao, I. Calizo, D. Teweldebrhan, F. Miao, C. N. Lau, *Nano Lett.* **2008**, *8*, 902.
[11] C. Lee, X. D. Wei, J. W. Kysar, J. Hone, *Science* **2008**, *321*, 385.
[12] N. Mohanty, V. Berry, *Nano Lett.* **2008**, *8*, 4469.
[13] F. Schedin, A. K. Geim, S. V. Morozov, E. W. Hill, P. Blake, M. I. Katsnelson, K. S. Novoselov, *Nat. Mater.* **2007**, *6*, 652.
[14] J. Liu, J. Tang, J. J. Gooding, *J. Mater. Chem.* **2012**, *22*, 12435.
[15] X. Huang, Z. Yin, S. Wu, X. Qi, Q. He, Q. Zhang, Q. Yan, F. Boey, H. Zhang, *Small* **2011**, *7*, 1876.
[16] W. Wei, X. Qu, *Small* **2012**, *8*, 2138.
[17] Z. Sun, D. K. James, J. M. Tour, *J. Phys. Chem. Lett.* **2011**, *2*, 2425.
[18] C. N. R. Rao, K. S. Subrahmanyam, H. S. S. Ramakrishna Matte, A. Govindaraj, *Mod. Phys. Lett. B* **2011**, *25*, 427.
[19] T. S. Sreeprasad, T. Pradeep, *Int. J. Mod. Phys. B* **2012**, *26*, 1242001.
[20] X. Huang, Z. Yin, S. Wu, X. Qi, Q. He, Q. Zhang, Q. Yan, F. Boey, H. Zhang, *Small* **2011**, *7*, 1876.
[21] O. C. Compton, S. T. Nguyen, *Small* **2010**, *6*, 711.
[22] L. Yan, Y. B. Zheng, F. Zhao, S. Li, X. Gao, B. Xu, P. S. Weiss, Y. Zhao, *Chem. Soc. Rev.* **2012**, *41*, 97.
[23] T. M. Swager, *ACS Macro Lett.* **2011**, *1*, 3.
[24] J. G. S. Elton, *New J. Phys.* **2012**, *14*, 043022.
[25] D. C. Elias, R. R. Nair, T. M. G. Mohiuddin, S. V. Morozov, P. Blake, M. P. Halsall, A. C. Ferrari, D. W. Boukhvalov, M. I. Katsnelson, A. K. Geim, K. S. Novoselov, *Science* **2009**, *323*, 610.
[26] P. Nguyen, V. Berry, *J. Phys. Chem. Lett.* **2012**, *3*, 1024.
[27] J. Xia, F. Chen, J. Li, N. Tao, *Nat. Nanotechnol.* **2009**, *4*, 505.
[28] S.-J. Sun, C.-Y. Lin, *Europhys. Lett.* **2011**, *96*, 10002.
[29] D. Wei, Y. Liu, Y. Wang, H. Zhang, L. Huang, G. Yu, *Nano Lett.* **2009**, *9*, 1752.
[30] G. Eda, Y. Y. Lin, C. Mattevi, H. Yamaguchi, H. A. Chen, I. S. Chen, C. W. Chen, M. Chhowalla, *Adv. Mater.* **2010**, *22*, 505.
[31] N. Mohanty, D. Moore, Z. Xu, T. S. Sreeprasad, A. Nagaraja, A. A. Rodriguez, V. Berry, *Nat. Commun.* **2012**, *3*, 844.
[32] I. Jung, D. A. Dikin, R. D. Piner, R. S. Ruoff, *Nano Lett.* **2008**, *8*, 4283.
[33] A. Cortijo, M. A. H. Vomediano, *Nuclear Phys. B* **2007**, *763*, 293.
[34] A. B. Kaiser, C. Gomez-Navarro, R. S. Sundaram, M. Burghard, K. Kern, *Nano Lett.* **2009**, *9*, 1787.
[35] T. Jayasekera, J. W. Mintmire, *Int. J. Quantum Chem.* **2007**, *107*, 3071.
[36] K. Jasuja, V. Berry, *ACS Nano* **2009**, *3*, 2358.
[37] M. Y. Han, B. Ozyilmaz, Y. B. Zhang, P. Kim, *Phys. Rev. Lett.* **2007**, *98*, 206805.
[38] M. I. Katsnelson, K. S. Novoselov, A. K. Geim, *Nat. Phys.* **2006**, *2*, 620.
[39] P. Huang, L. Jing, H. R. Zhu, X. Y. Gao, *J. Phys.: Condens. Matter* **2012**, *24*, 235305.
[40] J. Martin, N. Akerman, G. Ulbricht, T. Lohmann, J. H. Smet, K. von Klitzing, A. Yacoby, *Nat. Phys.* **2008**, *4*, 144.
[41] Q. H. Wang, Z. Jin, K. K. Kim, A. J. Hilmer, G. L. C. Paulus, C. J. Shih, M. H. Ham, J. D. Sanchez-Yamagishi, K. Watanabe, T. Taniguchi, J. Kong, P. Jarillo-Herrero, M. S. Strano, *Nat. Chem.* **2012**, *4*, 724.
[42] W. S. Hummers, R. E. Offeman, *J. Am. Chem. Soc.* **1958**, *80*, 1339.
[43] W. Gao, L. B. Alemany, L. Ci, P. M. Ajayan, *Nat. Chem.* **2009**, *1*, 403.
[44] D. R. Dreyer, S. Park, C. W. Bielawski, R. S. Ruoff, *Chem. Soc. Rev.* **2010**, *39*, 228.
[45] B. C. Brodie, *Phil. Trans. R. Soc. London* **1859**, *149*, 249.
[46] M. Trömel, M. Russ, *Angew. Chem.* **1987**, *99*, 1037.
[47] A. B. Bourlinos, D. Gournis, D. Petridis, T. Szabó, A. Szeri, I. Dékány, *Langmuir* **2003**, *19*, 6050.
[48] J. R. Lomeda, C. D. Doyle, D. V. Kosynkin, W. F. Hwang, J. M. Tour, *J. Am. Chem. Soc.* **2008**, *130*, 16201.
[49] S. Niyogi, E. Bekyarova, M. E. Itkis, J. L. McWilliams, M. A. Hamon, R. C. Haddon, *J. Am. Chem. Soc.* **2006**, *128*, 7720.

[50] Z. Liu, J. T. Robinson, X. Sun, H. Dai, *J. Am. Chem. Soc.* **2008**, *130*, 10876.
[51] X. D. Zhuang, Y. Chen, G. Liu, P. P. Li, C. X. Zhu, E. T. Kang, K. G. Noeh, B. Zhang, J. H. Zhu, Y. X. Li, *Adv. Mater.* **2010**, *22*, 1731.
[52] Y. Xu, Z. Liu, X. Zhang, Y. Wang, J. Tian, Y. Huang, Y. Ma, X. Zhang, Y. Chen, *Adv. Mater.* **2009**, *21*, 1275.
[53] J. Shen, B. Yan, M. Shi, H. Ma, N. Li, M. Ye, *J. Colloid Interface Sci.* **2011**, *356*, 543.
[54] N. Mohanty, V. Berry, *Nano Lett.* **2008**, *8*, 4469.
[55] N. Mohanty, M. Fahrenholtz, A. Nagaraja, D. Boyle, V. Berry, *Nano Lett.* **2011**, *11*, 1270.
[56] S. Stankovich, D. A. Dikin, G. H. B. Dommett, K. M. Kohlhaas, E. J. Zimney, E. A. Stach, R. D. Piner, S. T. Nguyen, R. S. Ruoff, *Nature* **2006**, *442*, 282.
[57] D. D. Zhang, S. Z. Zu, B. H. Han, *Carbon* **2009**, *47*, 2993.
[58] C. Xu, X. Wu, J. Zhu, X. Wang, *Carbon* **2008**, *46*, 386.
[59] C. Xu, X. Wang, J. Wang, H. Hu, L. Wan, *Chem. Phys. Lett.* **2010**, *498*, 162.
[60] H. J. Salavagione, M. ü. A. Gómez, G. Martínez, *Macromolecules* **2009**, *42*, 6331.
[61] Y. Matsuo, T. Tabata, T. Fukunaga, T. Fukutsuka, Y. Sugie, *Carbon* **2005**, *43*, 2875.
[62] T. Kuila, S. Bose, C. E. Hong, M. E. Uddin, P. Khanra, N. H. Kim, J. H. Lee, *Carbon* **2011**, *49*, 1033.
[63] J. Shen, M. Shi, H. Ma, B. Yan, N. Li, Y. Hu, M. Ye, *J. Colloid Interface Sci.* **2010**, *352*, 366.
[64] M. C. Hsiao, S. H. Liao, M. Y. Yen, P. I. Liu, N. W. Pu, C. A. Wang, C. C. Ma, *ACS Appl. Mater. Interfaces* **2010**, *2*, 3092.
[65] G. Wang, B. Wang, J. Park, J. Yang, X. Shen, J. Yao, *Carbon* **2009**, *47*, 68.
[66] C. Shan, H. Yang, D. Han, Q. Zhang, A. Ivaska, L. Niu, *Langmuir* **2009**, *25*, 12030.
[67] X. Sun, Z. Liu, K. Welsher, J. Robinson, A. Goodwin, S. Zaric, H. Dai, *Nano Res.* **2008**, *1*, 203.
[68] L. Q. Xu, W. J. Yang, K. G. Neoh, E. T. Kang, G. D. Fu, *Macromolecules* **2010**, *43*, 8336.
[69] T. A. Pham, N. A. Kumar, Y. T. Jeong, *Synthetic Metals* **2010**, *160*, 2028.
[70] S. M. Kang, S. Park, D. Kim, S. Y. Park, R. S. Ruoff, H. Lee, *Adv. Funct. Mater.* **2011**, *21*, 108.
[71] T. Kuila, P. Khanra, S. Bose, N. H. Kim, B.-C. Ku, B. Moon, J. H. Lee, *Nanotechnology* **2011**, *22*, 305710.
[72] H. Yang, F. Li, C. Shan, D. Han, Q. Zhang, L. Niu, A. Ivaska, *J. Mater. Chem.* **2009**, *19*, 4632.
[73] H. Yang, C. Shan, F. Li, D. Han, Q. Zhang, L. Niu, *Chem. Commun.* **2009**, 3880.
[74] B. K. Ahn, J. Sung, Y. Li, N. Kim, M. Ikenberry, K. Hohn, N. Mohanty, P. Nguyen, T. S. Sreeprasad, S. Kraft, V. Berry, X. S. Sun, *Adv. Mater.* **2012**, *24*, 2123.
[75] E. Bekyarova, M. E. Itkis, P. Ramesh, C. Berger, M. Sprinkle, W. A. de Heer, R. C. Haddon, *J. Am. Chem. Soc.* **2009**, *131*, 1336.
[76] Z. Sun, S. i. Kohama, Z. Zhang, J. Lomeda, J. Tour, *Nano Res.* **2010**, *3*, 117.
[77] Y. Si, E. T. Samulski, *Nano Lett.* **2008**, *8*, 1679.
[78] Y. Zhu, A. L. Higginbotham, J. M. Tour, *Chem. Mater.* **2009**, *21*, 5284.
[79] M. Fang, K. Wang, H. Lu, Y. Yang, S. Nutt, *J. Mater. Chem.* **2009**, *19*, 7098.
[80] V. H. Pham, T. V. Cuong, S. H. Hur, E. Oh, E. J. Kim, E. W. Shin, J. S. Chung, *J. Mater. Chem.* **2011**, *21*, 3371.
[81] S. Sarkar, E. Bekyarova, R. C. Haddon, *Acc. Chem. Res.* **2012**, *45*, 673.
[82] V. Georgakilas, A. B. Bourlinos, R. Zboril, T. A. Steriotis, P. Dallas, A. K. Stubos, C. Trapalis, *Chem. Commun.* **2010**, *46*, 1766.
[83] M. Quintana, K. Spyrou, M. Grzelczak, W. R. Browne, P. Rudolf, M. Prato, *ACS Nano* **2010**, *4*, 3527.
[84] J. Choi, K. j. Kim, B. Kim, H. Lee, S. Kim, *J. Phys. Chem. C* **2009**, *113*, 9433.
[85] X. Xu, Q. Luo, W. Lv, Y. Dong, Y. Lin, Q. Yang, A. Shen, D. Pang, J. Hu, J. Qin, Z. Li, *Macromol. Chem. Phys.* **2011**, *212*, 768.
[86] X. Zhong, J. Jin, S. Li, Z. Niu, W. Hu, R. Li, J. Ma, *Chem. Commun.* **2010**, *46*, 7340.
[87] S. P. Economopoulos, G. Rotas, Y. Miyata, H. Shinohara, N. Tagmatarchis, *ACS Nano* **2010**, *4*, 7499.
[88] S. Vadukumpully, J. Gupta, Y. Zhang, G. Q. Xu, S. Valiyaveettil, *Nanoscale* **2011**, *3*, 303.
[89] S. Lebegue, M. Klintenberg, O. Eriksson, M. I. Katsnelson, *Phys. Rev. B* **2009**, *79*, 245117.
[90] R. Balog, B. Jorgensen, L. Nilsson, M. Andersen, E. Rienks, M. Bianchi, M. Fanetti, E. Laegsgaard, A. Baraldi, S. Lizzit, Z. Sljivancanin, F. Besenbacher, B. Hammer, T. G. Pedersen, P. Hofmann, L. Hornekaer, *Nat. Mater.* **2010**, *9*, 315.
[91] J. T. Robinson, J. S. Burgess, C. E. Junkermeier, S. C. Badescu, T. L. Reinecke, F. K. Perkins, M. K. Zalalutdniov, J. W. Baldwin, J. C. Culbertson, P. E. Sheehan, E. S. Snow, *Nano Lett.* **2010**, *10*, 3001.
[92] R. R. Nair, W. Ren, R. Jall, I. Riaz, V. G. Kravets, L. Britnell, P. Blake, F. Schedin, A. S. Mayorov, S. Yuan, M. I. Katsnelson, H. M. Cheng, W. Strupinski, L. G. Bulusheva, A. V. Okotrub, I. V. Grigorieva, A. N. Grigorenko, K. S. Novoselov, A. K. Geim, *Small* **2010**, *6*, 2877.
[93] S. H. Cheng, K. Zou, F. Okino, H. R. Gutierrez, A. Gupta, N. Shen, P. C. Eklund, J. O. Sofo, J. Zhu, *Phys. Rev. B* **2010**, *81*, 205435.
[94] B. Li, L. Zhou, D. Wu, H. Peng, K. Yan, Y. Zhou, Z. Liu, *ACS Nano* **2011**, *5*, 5957.
[95] J. Wu, L. Xie, Y. Li, H. Wang, Y. Ouyang, J. Guo, H. Dai, *J. Am. Chem. Soc.* **2011**, *133*, 19668.
[96] G. Imamura, K. Saiki, *J. Phys. Chem. C* **2011**, *115*, 10000.
[97] B. Guo, Q. Liu, E. Chen, H. Zhu, L. Fang, J. R. Gong, *Nano Lett.* **2010**, *10*, 4975.
[98] T. Wu, H. Shen, L. Sun, B. Cheng, B. Liu, J. Shen, *New J. Chem.* **2012**, *36*, 1385.
[99] I. Gierz, C. Riedl, U. Starke, C. R. Ast, K. Kern, *Nano Lett.* **2008**, *8*, 4603.
[100] A. Bostwick, T. Ohta, T. Seyller, K. Horn, E. Rotenberg, *Nat. Phys.* **2007**, *3*, 36.
[101] T. Ohta, A. Bostwick, T. Seyller, K. Horn, E. Rotenberg, *Science* **2006**, *313*, 951.
[102] D. M. Chen, P. M. Shenai, Y. Zhao, *Phys. Chem. Chem. Phys.* **2011**, *13*, 1515.
[103] F. Yavari, C. Kritzinger, C. Gaire, L. Song, H. Gulapalli, T. Borca-Tasciuc, P. M. Ajayan, N. Koratkar, *Small* **2010**, *6*, 2535.
[104] H. Lee, S. Yang, J. Choi, Y. Park, S. Kim, *J. Phys. Chem. C* **2011**, *115*, 18736.
[105] X. L. Li, X. R. Wang, L. Zhang, S. W. Lee, H. J. Dai, *Science* **2008**, *319*, 1229.
[106] Y. Xu, H. Bai, G. Lu, C. Li, G. Shi, *J. Am. Chem. Soc.* **2008**, *130*, 5856.
[107] Q. Su, S. Pang, V. Alijani, C. Li, X. Feng, K. Müllen, *Adv. Mater.* **2009**, *21*, 3191.
[108] W. Tu, J. Lei, S. Zhang, H. Ju, *Chem. Eur. J.* **2010**, *16*, 10771.
[109] Y. Xu, H. Bai, G. Lu, C. Li, G. Shi, *J. Am. Chem. Soc.* **2008**, *130*, 5856.
[110] Y. Xu, L. Zhao, H. Bai, W. Hong, C. Li, G. Shi, *J. Am. Chem. Soc.* **2009**, *131*, 13490.
[111] A. Ghosh, K. V. Rao, S. George, C. N. R. Rao, *Chem. Eur. J.* **2010**, *16*, 2700.
[112] S. Park, N. Mohanty, J. W. Suk, A. Nagaraja, J. An, R. D. Piner, W. Cai, D. R. Dreyer, V. Berry, R. S. Ruoff, *Adv. Mater.* **2010**, *22*, 1736.

[113] Y. T. Liang, M. C. Hersam, *J. Am. Chem. Soc.* **2010**, *132*, 17661.
[114] X. Li, G. Zhang, X. Bai, X. Sun, X. Wang, E. Wang, H. Dai, *Nat. Nanotechnol.* **2008**, *3*, 538.
[115] X. Li, X. Wang, L. Zhang, S. Lee, H. Dai, *Science* **2008**, *319*, 1229.
[116] T. Ramanathan, A. A. Abdala, S. Stankovich, D. A. Dikin, M. Herrera-Alonso, R. D. Piner, D. H. Adamson, H. C. Schniepp, X. Chen, R. S. Ruoff, S. T. Nguyen, I. A. Aksay, R. K. Prud'homme, L. C. Brinson, *Nat. Nanotechnol.* **2008**, *3*, 327.
[117] Y. Wang, D. Kurunthu, G. W. Scott, C. J. Bardeen, *J. Phys. Chem. C* **2010**, *114*, 4153.
[118] M. Kim, N. S. Safron, C. Huang, M. S. Arnold, P. Gopalan, *Nano Lett.* **2011**, *12*, 182.
[119] J. P. Rourke, P. A. Pandey, J. J. Moore, M. Bates, I. A. Kinloch, R. J. Young, N. R. Wilson, *Angew. Chem. Int. Ed.* **2011**, *50*, 3173.
[120] F. Schedin, A. K. Geim, S. V. Morozov, E. W. Hill, P. Blake, M. I. Katsnelson, K. S. Novoselov, *Nat. Mater.* **2007**, *6*, 652.
[121] M. Gautam, A. H. Jayatissa, *Mater. Sci. Engin. C* **2011**, *31*, 1405.
[122] I. Jung, D. Dikin, S. Park, W. Cai, S. L. Mielke, R. S. Ruoff, *J. Phys. Chem. C* **2008**, *112*, 20264.
[123] G. H. Lu, L. E. Ocola, J. H. Chen, *Appl. Phys. Lett.* **2009**, *94*, 083111.
[124] M. Qazi, T. Vogt, G. Koley, *Appl. Phys. Lett.* **2007**, *91*.
[125] H. Sukju, H. C. Joon, L. Juwhan, K. K. Whan, S. Hyunjin, J. Y. Choi, J. H. Choi, Y. L. Sang, J. M. Kim, H. K. Jae, L. Seok, C. J. Seong, presented at Nanotechnology Materials and Devices Conference (NMDC), **2010** IEEE.
[126] S. Rumyantsev, G. Liu, M. S. Shur, R. A. Potyrailo, A. A. Balandin, *Nano Lett.* **2012**, *12*, 2294.
[127] J. D. Fowler, M. J. Allen, V. C. Tung, Y. Yang, R. B. Kaner, B. H. Weiller, *ACS Nano* **2009**, *3*, 301.
[128] F. Yavari, Z. Chen, A. V. Thomas, W. Ren, H. M. Cheng, N. Koratkar, *Sci. Rep.* **2011**, *1*.
[129] G. Lu, S. Park, K. Yu, R. S. Ruoff, L. E. Ocola, D. Rosenmann, J. Chen, *ACS Nano* **2011**, *5*, 1154.
[130] G. Konstantatos, M. Badioli, L. Gaudreau, J. Osmond, M. Bernechea, F. P. G. de Arquer, F. Gatti, F. H. L. Koppens, *Nat. Nanotechnol.* **2012**, *7*, 363.
[131] D. Zhang, L. Gan, Y. Cao, Q. Wang, L. Qi, X. Guo, *Adv. Mater.* **2012**, *24*, 2715.
[132] Z. Fang, Z. Liu, Y. Wang, P. M. Ajayan, P. Nordlander, N. J. Halas, *Nano Lett.* **2012**, *12*, 3808.
[133] Q. H. Wang, Z. Jin, K. K. Kim, A. J. Hilmer, G. L. C. Paulus, C. J. Shih, M. H. Ham, J. D. Sanchez-Yamagishi, K. Watanabe, T. Taniguchi, J. Kong, P. Jarillo-Herrero, M. S. Strano, *Nat. Chem.* **2012**, *4*, 724.

Received: September 6, 2012
Published online: November 21, 2012